A Location-based Self-Optimizing Algorithm for the Inter-RAT Handover Parameters

Ahmad Awada and Bernhard Wegmann
Nokia Siemens Networks
Munich, Germany
Emails: {ahmad.awada.ext; bernhard.wegmann}
@nsn.com

Ingo Viering
Nomor Research GmbH
Munich, Germany
Email: viering@nomor.de

Anja Klein
Technische Universität Darmstadt
Communications Engineering Lab
Darmstadt, Germany
Email: a.klein@nt.tu-darmstadt.de

***Abstract*—The Long Term Evolution (LTE) is a new radio access technology (RAT) which is currently being deployed on top of the second generation (2G) or third generation (3G) mobile networks. As a result, user equipments (UEs) will be handed over from one RAT to another. To improve the robustness of the inter-RAT handovers and reduce cost, self-organizing networks (SONs) are used to configure the inter-RAT handover thresholds in an automatic and autonomous way replacing the current manual based optimization methods. The handover thresholds can be configured cell-specifically or cell-pair specifically where a dedicated handover threshold is configured with respect to each target cell of handover. However, both optimization paradigms can fail to resolve all mobility failure events in some cells where radio conditions are not stationary along the cell border. In this paper, we propose a new paradigm for configuring and optimizing the inter-RAT handover thresholds based on the locations of UEs in the cell. Simulation results show that the new paradigm outperforms cell-specific and cell-pair specific schemes by resolving additional numbers of mobility failures.**

***Index Terms*—Location-based optimization, self-organizing network, inter-RAT mobility robustness optimization.**

I. Introduction

Robustness of the inter-RAT handovers depends mainly on the configuration of the handover thresholds. Currently, the handover thresholds are optimized manually with the aid of network planning tools, drive tests and analysis of experts [1]. This manual optimization is inconvenient for the mobile operators as it requires permanent human intervention and increases as well the operational expenditures (OPEX). To overcome this burden, self-organizing network (SON) is foreseen to optimize automatically and autonomously the handover thresholds [2].

A SON-based algorithm for inter-RAT mobility robustness optimization (MRO) is proposed in [3] to optimize the handover thresholds of Long Term Evolution (LTE) and third generation (3G) cells in a cell-specific way, i.e., the handover thresholds are not differentiated with respect to the neighboring target cell of handover. The problem with the cell-specific (CS) MRO paradigm is that the optimized handover setting results from averaging over all target cells, and therefore some of the mobility failure events cannot be resolved. This limitation has been addressed in [4] and the algorithm has been extended to allow cell-pair specific (CPS) optimization using cell-individual offsets to provide a dedicated handover threshold value with respect to each target cell of handover. Though CPS MRO paradigm provides more degrees of freedom to address different radio conditions towards different target cells, it can still fail since radio conditions can be even not stationary along the border of the same target cell of handover, in particular in the inter-RAT case where the area of potential handover is large. In this paper, we propose a new location-based (LB) MRO paradigm which provides finer granularity than CPS MRO. The mobility failure events in a cell are collected per small areas and the user equipments (UEs) apply specific handover threshold values when they approach those areas.

The paper is organized as follows. The inter-RAT handover thresholds are explained in section II. The key performance indicators (KPIs) which are used for inter-RAT scenario are described in III. The CS and CPS MRO paradigms are reviewed in section IV. The LB MRO algorithm is explained in section V. The inter-RAT simulation scenario with overlaying LTE and 3G networks is given in section VI. The performances of CS, CPS and LB MRO paradigms are compared in section VII. The paper is then concluded in section VIII.

II. Inter-RAT Handover Thresholds

In this section, we define the handover thresholds for the inter-RAT scenario after giving few definitions.

The neighboring cells of a cell c which belong to a different RAT are denoted by the set $\mathcal{L}_c$. A UE u served by a cell c measures at time instant t a received signal $M_{u,c}(t)$ from the serving cell c and a signal $M_{u,c_0}(t)$ from a target cell $c_0 \in \mathcal{L}_c$. In this work, $M_{u,c}(t)$ and $M_{u,c_0}(t)$ are signal-strength based measurements expressed in dBm [5].

The reporting of the measurements $M_{u,c}(t)$ or $M_{u,c_0}(t)$ to the serving base station can be either periodic or event triggered. For an event triggered report, the UE sends its measurement report when a certain condition, called also the entering condition of the measurement event, is fulfilled for a time-to-trigger (TTT) time interval denoted by T_{T}. The entering condition of the dual threshold measurement event, normally used for inter-RAT scenario, is fulfilled when the measured signal $M_{u,c}(t)$ of a UE u connected to the serving cell c falls below a predefined serving threshold and the measured signal $M_{u,c_0}(t)$ of the neighboring target cell c_0

is higher than a second target threshold. These two thresholds are to be optimized by the SON-based algorithm.

III. The KPIs for Inter-RAT Scenario

The inter-RAT mobility failure events are classified into failure types or so-called KPIs. In accordance to the KPIs defined for the intra-LTE case [2], two categories of KPIs are defined for the inter-RAT scenario: The first captures inter-RAT radio link failures (RLFs) and the second the unwanted and costly inter-RAT handovers.

A. Types of Inter-RAT Handover Failure

The three types of inter-RAT handover failure are as follows:

1) *Too late inter-RAT handover (TLH)*: The UE drops before a handover is initiated or concluded from one RAT to another and the UE reconnects to a cell in a RAT which is different from that of the previously serving cell. In inter-RAT case, there are two thresholds controlling each measurement event and therefore, two types of TLHs exist [3]: A TLH due to the misconfiguration of the serving or target threshold is denoted by TLH-S or TLH-T, respectively. Our proposal to differentiate between the two types of TLHs has been recently adopted by LTE Release 11 (Rel. 11) standard [6].
2) *Too early inter-RAT handover (TEH)*: The UE is successfully handed over from cell A to another cell B of a different RAT. Shortly after, an RLF happens and the UE reconnects to the previous RAT either to the same cell A or to a different one.
3) *Inter-RAT handover to wrong cell (HWC)*: The UE is successfully handed over from cell A to another cell B of a different RAT. Shortly after, an RLF happens and the UE reconnects to a third cell C belonging to the same RAT as cell B.

B. Costly Inter-RAT Handovers

There are two types of costly inter-RAT handovers:

1) *Ping-pong (PP)*: The UE is handed over to a cell of a different RAT and within a time interval T_{PP}, the UE is handed over back to the same cell or to a different cell of the previous RAT.
2) *Unnecessary handover (UH)*: The UE is handed over from a high priority RAT (LTE in our case) to a low priority RAT (3G) even though the signal quality of the previous LTE cell is still good enough [7].

IV. CS and CPS Optimization Paradigms

In this section, we briefly review the CS and CPS MRO paradigms for the inter-RAT handover thresholds.

A. CS MRO Paradigm

In CS MRO paradigm, a cell c can only configure two values for the handover thresholds, denoted by $S_c^{(\text{thr})}$ and $T_c^{(\text{thr})}$, irrespective of the target cell. That is all the UEs served by cell c apply the same handover thresholds when handing over to any target cell, see Fig. 1(a). The CS MRO paradigm is convenient since it handles few numbers of parameter settings and counters and, therefore less complex compared to CPS MRO paradigm. However, CS MRO paradigm fails when the mobility failure events occurring with respect to a target cell $c_0' \in \mathcal{L}_c$ require an increase in the value of the handover threshold, e.g., $T_c^{(\text{thr})}$, whereas those occurring with respect to another target cell $c_0'' \in \mathcal{L}_c$ require a decrease in the value of the same handover threshold. In this case, the CS MRO paradigm cannot react and a CPS MRO paradigm is needed to tackle the latter problem.

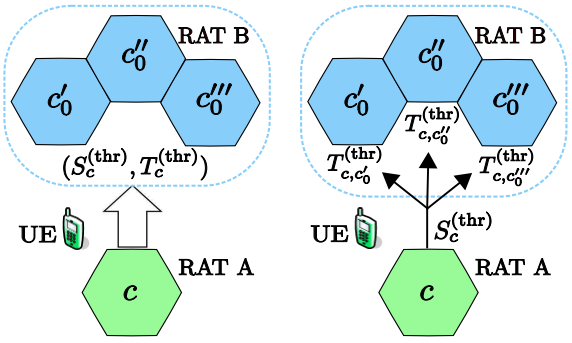

(a) CS MRO paradigm. (b) CPS MRO paradigm.

Fig. 1. The two CS and CPS MRO paradigms.

B. CPS MRO Paradigm

Unlike the CS MRO paradigm, different values of the handover thresholds can be configured with respect to the each target cell. Investigations in [4] have shown that configuring only the target handover threshold in CPS manner is beneficial, i.e., CS serving threshold $S_c^{(\text{thr})}$ and CPS target threshold $T_{c,c_0}^{(\text{thr})}$, as depicted in Fig. 1(b) where $T_c^{(\text{thr})}$ is set differently with respect to each target cell. However, the resolution of the CPS MRO paradigm might be too coarse to isolate problematic areas with different failure types: For instance, when two types of mobility failure events in cell c require an increase and a decrease, respectively in $S_c^{(\text{thr})}$ threshold or when the mobility failure events occurring with respect to the same target cell c_0 require contradicting actions to be performed on the same threshold $T_{c,c_0}^{(\text{thr})}$. To address these two limitations, more degrees of freedom are needed when configuring the handover thresholds and one of them is the location of the UEs in the network.

V. Description of the LB MRO Algorithm for the Inter-RAT Handover Thresholds

In this section, we describe the main components of the LB MRO algorithm for the inter-RAT handover thresholds which is depicted in Fig. 2 and its limitations.

A. Network Root Cause Analysis

The 3rd Generation Partnership Project (3GPP) has specified the root cause analysis procedure which descries the responsible cell having caused the mobility failure event due

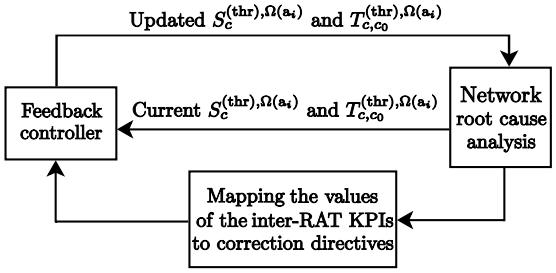

Fig. 2. Description of the location-based optimization loop for the inter-RAT handover thresholds.

to misconfigured handover thresholds. New values of the KPIs are counted by each cell during each KPI collection period of duration T_{KPI}.

In order to count the mobility failure events per area, the coverage area of a cell c is decomposed into a grid of small square areas a_i. The side length of the square area is d. The higher the value of d, the larger the area is, see Fig. 3. The center of each area a_i is located by the vector $\vec{\text{a}}_{i,c}$. We denote the location of a mobility failure event j occurring in cell c with respect to neighboring target cell c_0 by the vector $\vec{x}_{c,c_0}^{(j)}$. A mobility failure event j occurring in cell c with respect to neighboring target cell c_0 is assigned to the closest area a_{i^*} where

$$i^* = \min_i \|\vec{\text{a}}_{i,c} - \vec{x}_{c,c_0}^{(j)}\|^2. \quad (1)$$

The values of the KPIs: TLH-S, TLH-T, TEHs, HWC, PPs and UHs, collected in each area a_i of cell c with respect to target cell c_0, are denoted by $N_{c,c_0}^{\text{TLH-S},\text{a}_i}$, $N_{c,c_0}^{\text{TLH-T},\text{a}_i}$, $N_{c,c_0}^{\text{TEH},\text{a}_i}$, $N_{c,c_0}^{\text{HWC},\text{a}_i}$, $N_{c,c_0}^{\text{PP},\text{a}_i}$ and $N_{c,c_0}^{\text{UH},\text{a}_i}$, respectively. For clarity, an illustrative example is depicted in Fig. 3 for cell c.

In each area of the cell, either one or multiple types of mobility failure events exist, e.g., blue for TLH-S, or no failures at all, i.e., white squares. For all the areas with no mobility failure events, default values for the handover thresholds are configured by the base station. On the other hand, dedicated handover threshold values are assigned for all the other areas having mobility failure events and these are optimized by the LB MRO algorithm.

Each UE is configured by the serving cell with a location specific measurement configuration map which contains the handover thresholds of all the areas inside the cell. A UE approaching an area a_i should apply its corresponding handover thresholds a head of time before it experiences the same mobility failures which had occurred before in area a_i. Therefore, the UE applies the handover thresholds if it is inside the area a_i or in its proximity. Consequently, we denote the set of all the locations where the UE applies the handover thresholds of area a_i by $\Omega(\text{a}_i)$.

The serving cell configures $\Omega(\text{a}_i)$ and its definition depends on the type of the mobility failures in each area. For instance, a UE approaching an area a_i having TLHs should apply its corresponding handover thresholds early enough so that the entering condition can be fulfilled for T_{T} time interval before it fails. On the other hand, a UE approaching an area a_i having

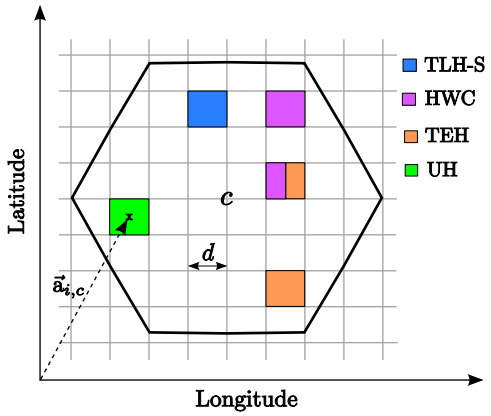

Fig. 3. Classifying the mobility failure events per small square areas with side length d.

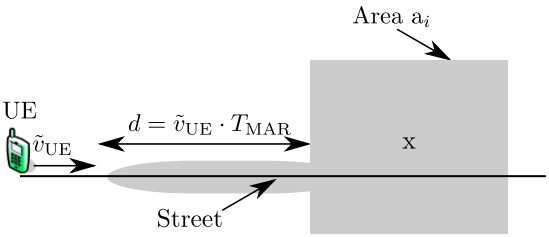

$\Omega(\text{a}_i)$: Gray area.

Fig. 4. The set of all the locations $\Omega(\text{a}_i)$ where the UE applies the handover thresholds of area a_i.

TEHs, HWC, PPs or UHs can avoid the handover if it applies the corresponding handover thresholds just before it enters the area a_i. An example of the definition of $\Omega(\text{a}_i)$ used in this work is depicted in Fig. 4. The figure shows a UE moving with a certain estimated velocity, denoted by $\tilde{v}_{\text{UE}}$, on a street passing through an area a_i. The UE starts to apply the handover thresholds when it is $d = \tilde{v}_{\text{UE}} \cdot T_{\text{MAR}}$ meters away from area a_i where T_{MAR} is the time margin configured by the serving cell depending on the type of mobility failures in a_i. In this work, T_{MAR} of areas having TLH-S or TLH-T is set to 3 seconds (s) whereas it is set to 0.5 s for all other areas having TEHs, HWC, PPs or UHs. We denote the serving and target thresholds configured by a cell c with respect to target cell c_0 for a UE located in $\Omega(\text{a}_i)$ by $S_c^{(\text{thr}),\Omega(\text{a}_i)}$ and $T_{c,c_0}^{(\text{thr}),\Omega(\text{a}_i)}$, respectively. The thresholds $S_c^{(\text{thr}),\Omega(\text{a}_i)}$ and $T_{c,c_0}^{(\text{thr}),\Omega(\text{a}_i)}$ are defined here as CS and CPS, respectively.

B. Mapping the Values of the Inter-RAT KPIs to Correction Directives

After each KPI collection period, the values of the KPIs of each area a_i are mapped into four new values, denoted by correction directives, which are defined as follows: $S_c^{(+),\text{a}_i}$ and $S_c^{(-),\text{a}_i}$ are the numbers of mobility failure events which require an increase and a decrease, respectively, in $S_c^{(\text{thr}),\Omega(\text{a}_i)}$, and $T_{c,c_0}^{(+),\text{a}_i}$ and $T_{c,c_0}^{(-),\text{a}_i}$ are the numbers of mobility failure events which require an increase and a decrease, respectively, in $T_{c,c_0}^{(\text{thr}),\Omega(\text{a}_i)}$, see Fig. 5. In case of a 3G cell, the value of

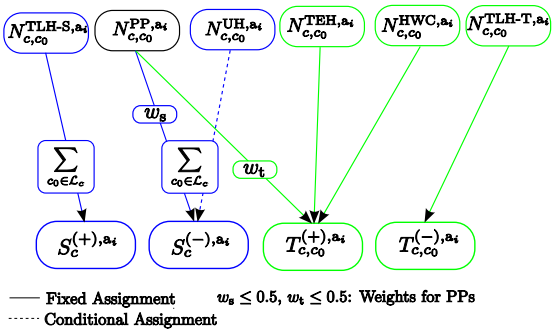

Fig. 5. Mapping the values of the KPIs into four new correction directives.

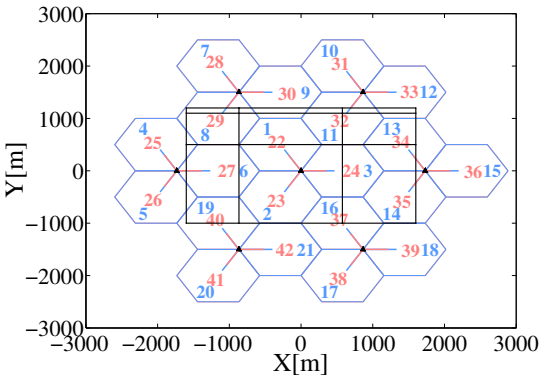

Fig. 6. An LTE network (blue) co-sited with a 3G network (red). The streets are shown in black.

UH KPI $N_{c,c_0}^{\mathrm{UH},\mathrm{a}_i}$ does not exist and is excluded. The mapping between the values of the KPIs and the correction directives has been discussed in [3]. The numbers of PPs are weighted using w_s and w_t in case the mobile operators want to give higher priority for RLF related KPIs. Moreover, among the assignments there is one which is conditional: $N_{c,c_0}^{\mathrm{UH},\mathrm{a}_i}$ is assigned to $S_c^{(-),\mathrm{a}_i}$ only when there are no TLHs in the cell, i.e., the coverage of the LTE cell is increased only when no TLHs exist.

C. Feedback Controller

The handover thresholds of each area a_i are updated based on the magnitudes of its corresponding correction directives provided that they are above a certain threshold at all. This condition is necessary to avoid reacting on insignificant numbers of failures or so-called outliers. The threshold $S_c^{(\mathrm{thr}),\Omega(\mathrm{a}_i)}$ is increased if $S_c^{(+),\mathrm{a}_i} \gg S_c^{(-),\mathrm{a}_i}$, decreased if $S_c^{(+),\mathrm{a}_i} \ll S_c^{(-),\mathrm{a}_i}$ and not modified if $S_c^{(+),\mathrm{a}_i} \approx S_c^{(-),\mathrm{a}_i}$, i.e., in this case the correction directives would most likely start to oscillate if $S_c^{(\mathrm{thr}),\Omega(\mathrm{a}_i)}$ is updated. The same concept applies for the target threshold $T_{c,c_0}^{(\mathrm{thr}),\Omega(\mathrm{a}_i)}$. For the sake of stability, the step size of increase or decrease that needs to be applied for each handover threshold is determined by the feedback controller which is discussed in details in [3].

D. Limitations of the Location Based Inter-RAT MRO

The proposed LB MRO algorithm has two limitations when optimizing the inter-RAT handover thresholds. The first one is when inside an area a_i, $S_c^{(+),\mathrm{a}_i} \approx S_c^{(-),\mathrm{a}_i}$ or $T_{c,c_0}^{(+),\mathrm{a}_i} \approx T_{c,c_0}^{(-),\mathrm{a}_i}$. This situation is unlikely to occur if the areas are small, i.e., small value of d. The second limitation is when $\Omega(\mathrm{a}_i)$ of area a_i intersects with $\Omega(\mathrm{a}_{i'})$ of a different area $\mathrm{a}_{i'}$ requiring different handover thresholds, i.e., $\Omega(\mathrm{a}_i) \cap \Omega(\mathrm{a}_{i'}) \neq \phi$. In this case, the UE can be configured by either the handover thresholds of area a_i or $\mathrm{a}_{i'}$.

VI. Simulation Scenario and Parameters

In this section, the simulation scenario is presented along with the simulation parameters.

The scenario used to evaluate the performances of CS, CPS and LB MRO paradigms is shown in Fig. 6. The scenario consists of 21 LTE cells co-sited with other 21 3G cells.

TABLE I
The Network Simulation Parameters.

Parameter	Assumptions
Carrier frequency	LTE: 2.6 GHz and 3G: 2.1 GHz
System bandwidth	LTE: 10 MHz and 3G: 5 MHz
Total transmit power	LTE: 40 W and 3G: 20 W
Shadowing	Standard deviation = 8 dB Decorrelation distance = 50 m
Fast Fading	2-tap Rayleigh fading channel
Noise Power	-174 dB/Hz + $10 \cdot \log_{10}(B\ [\mathrm{Hz}]) + 7$
Traffic model	Full buffer
T_T	0.1 s
T_KPI	150 s
T_PP	3 s

The identification numbers 1 to 21 (blue) are used for LTE cells and 22 to 42 for 3G cells (red). The total number of UEs in the network is set to 1010 distributed as follows: 5 background UEs moving randomly in each cell and 800 UEs moving on streets shown in black, see Fig. 6. The UEs located on the streets are uniformly distributed and select randomly a direction at every intersection. The speed of the background UEs is fixed to 3 km/h whereas the speed of the UEs moving on the street is varied in each simulation result and set to 30 km/h, 60 km/h, 90 km/h and 120 km/h.

The current network planning and optimization methods provide normally an initial fixed network-wide handover thresholds for all cells. For this purpose, a parameter sweep of a range of the handover thresholds is performed and the following best fixed setting for the handover thresholds is selected: $(S_c^{(\mathrm{thr}),\Omega(\mathrm{a}_i)}, T_{c,c_0}^{(\mathrm{thr}),\Omega(\mathrm{a}_i)}) = (-121, -100)$ dBm for LTE cells and $(S_c^{(\mathrm{thr}),\Omega(\mathrm{a}_i)}, T_{c,c_0}^{(\mathrm{thr}),\Omega(\mathrm{a}_i)}) = (-106, -115)$ dBm for 3G cells. The latter setting is denoted by "Reference" and is used to benchmark the performance of the different inter-RAT MRO paradigms. The weights w_s and w_t of PPs are set in this work to 0.5, i.e., a PP has the same weight of a RLF. The side length of the square areas is set to $d = 10$ m. The rest of the simulation parameters are summarized in Table I.

VII. Simulation Results

In this section, we compare the performances of CS, CPS and LB inter-RAT MRO paradigms.

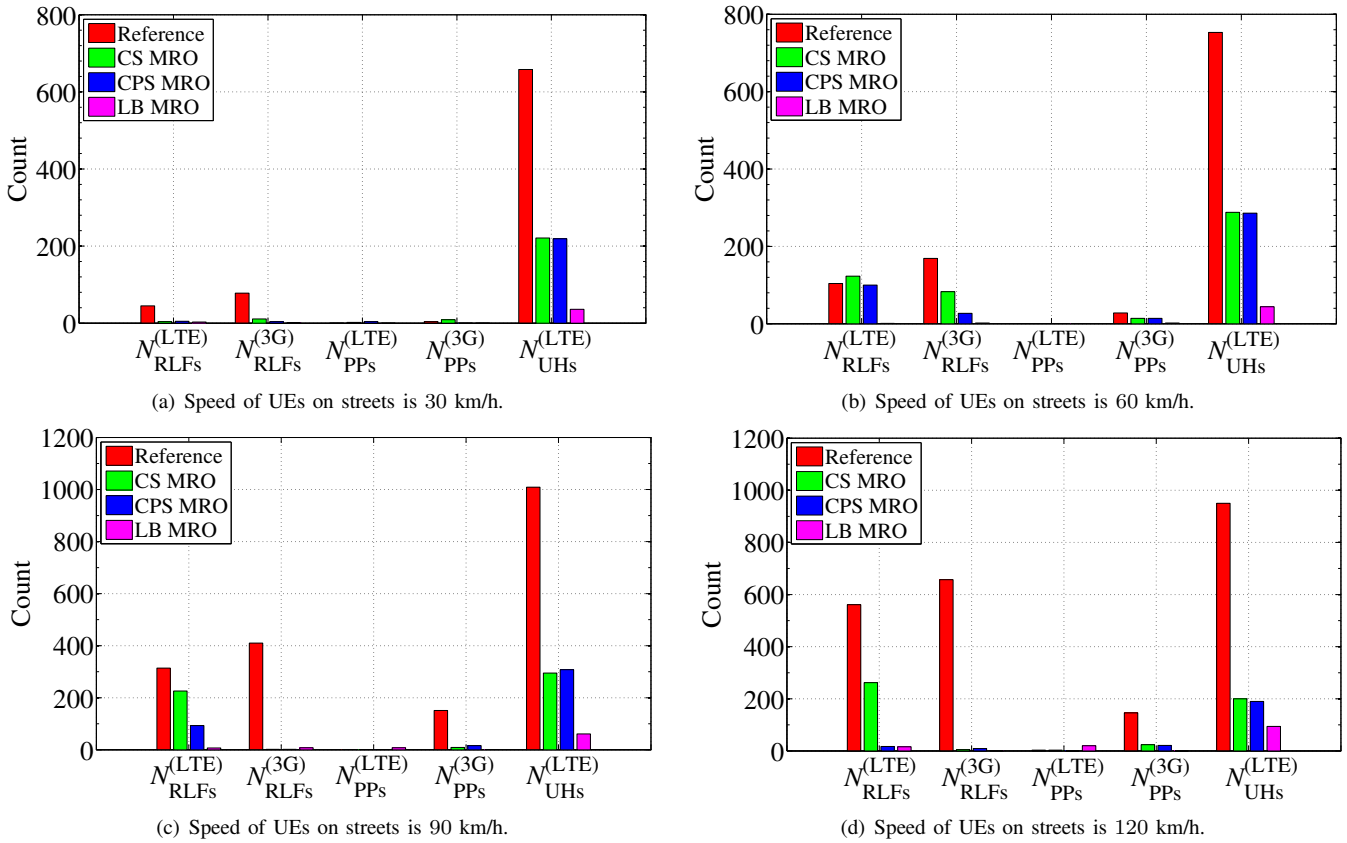

(a) Speed of UEs on streets is 30 km/h.

(b) Speed of UEs on streets is 60 km/h.

(c) Speed of UEs on streets is 90 km/h.

(d) Speed of UEs on streets is 120 km/h.

Fig. 7. Performance comparison between CS, CPS and LB inter-RAT MRO paradigms for different UE speeds.

The total number of RLFs, PPs and UHs in LTE network is denoted by $N^{(LTE)}_{RLFs}$, $N^{(LTE)}_{PPs}$ and $N^{(LTE)}_{UHs}$, respectively. Similarly, we denote the total number of RLFs and PPs in 3G network by $N^{(3G)}_{RLFs}$, $N^{(3G)}_{PPs}$, respectively. The results obtained by CS, CPS and LB inter-RAT MRO paradigms are denoted by "CS MRO", "CPS MRO" and "LB MRO", respectively.

In Fig. 7, we compare the performances of CS, CPS and LB MRO paradigms for different UE speeds. For a speed of 30 km/h, the three different inter-RAT MRO paradigms achieve the same performance in RLFs and PPs. However, $N^{(LTE)}_{UHs}$ of CS, CPS and LB MRO is 66.4%, 66.7% and 94.5%, respectively, lower than that of Reference. As for the speed of 60 km/h, LB MRO resolves completely the number of LTE RLFs in contrast to CS and CPS MRO paradigms which fail to improve the performance compared to Reference. Moreover, $N^{(LTE)}_{UHs}$ of CS, CPS and LB MRO is 61.8%, 62% and 94.1%, respectively, lower than that of Reference. A similar performance is also shown in Fig. 7(c) where LB MRO achieves lower numbers of $N^{(LTE)}_{RLFs}$ and $N^{(LTE)}_{UHs}$ than those of CS and CPS paradigms. For a speed of 120 km/h, both CPS and LB MRO paradigms resolve all RLFs and PPs. However, LB MRO achieves roughly a gain of 50% in $N^{(LTE)}_{UHs}$ compared to that of CS or CPS MRO. Therefore, the results show that LB MRO outperforms CS and CPS MRO and resolves most of the mobility problems in LTE and 3G networks.

To highlight the advantage of LB MRO over CPS MRO paradigm in reducing $N^{(LTE)}_{RLFs}$ and $N^{(LTE)}_{UHs}$, we show in Fig. 8 the number of RLFs and UHs in LTE cells as a function of the KPI collection period for the UE speed of 60 km/h. For clarity, we show in Fig. 8(b) only a subset of the LTE cells having UHs problems. It is shown in Fig. 8(a) that only cell 11 has initially RLF problems. This is because the initial setting of the handover thresholds has been already optimized by selecting the best network-wide setting which we have denoted by Reference. The CPS MRO paradigm fails to resolve the number of RLFs of cell 11 as two different types of mobility failures occurring with respect to the same 3G target cell $c_0 = 32$ require two contradicting handover threshold actions, i.e., numbers of mobility failures requiring an increase and a decrease in $T^{(\text{thr})}_{c,c_0}$ threshold are comparable, see section V-C. Moreover, it is shown in Fig. 8(b) that CPS MRO paradigm did not react on UHs of cell 11 since it has already TLHs failures which have higher priority than UHs, see Fig. 5. On the other hand, LB MRO paradigm is able to resolve $N^{(LTE)}_{RLFs}$ and $N^{(LTE)}_{UHs}$ of cell 11 by exploiting the locations of the mobility failures and assigning different handover threshold values for each area of the cell.

The optimized values of $S^{(\text{thr}),\Omega(\text{a}_i)}_{c}$ and $T^{(\text{thr}),\Omega(\text{a}_i)}_{c,c_0}$ thresholds for each area a_i of cell $c = 11$ are shown in Fig. 9 with respect to target cell $c_0 = 32$. The white color denotes the initial configured value of $S^{(\text{thr}),\Omega(\text{a}_i)}_{c} = -121$ dBm and $T^{(\text{thr}),\Omega(\text{a}_i)}_{c,c_0} = -100$ dBm. It is shown in Fig. 9(a) that areas

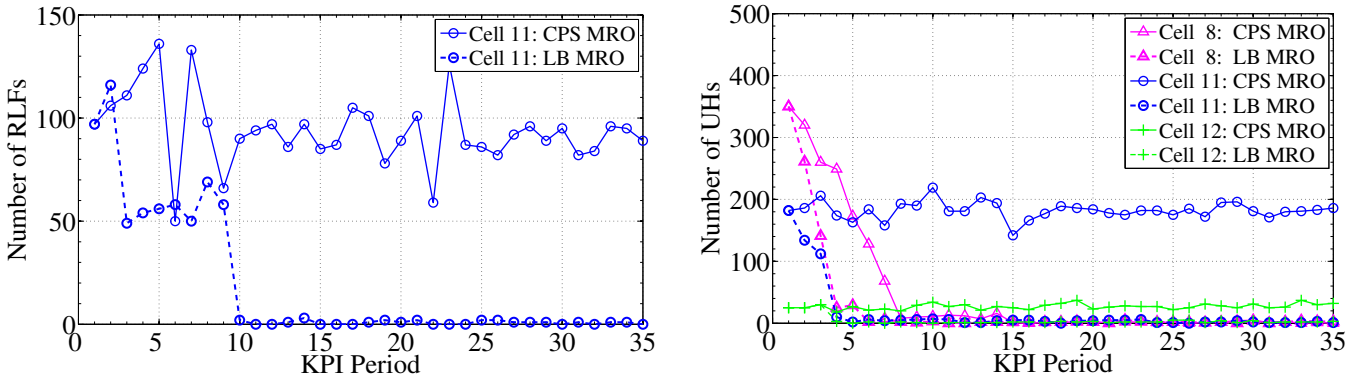

(a) LTE cell having RLF problems.

(b) A subset of LTE cells having UH problems.

Fig. 8. Performance comparison between CPS and LB inter-RAT MRO paradigms with respect to number of RLFs and UHs in LTE cells. Speed of UEs on streets is 60 km/h.

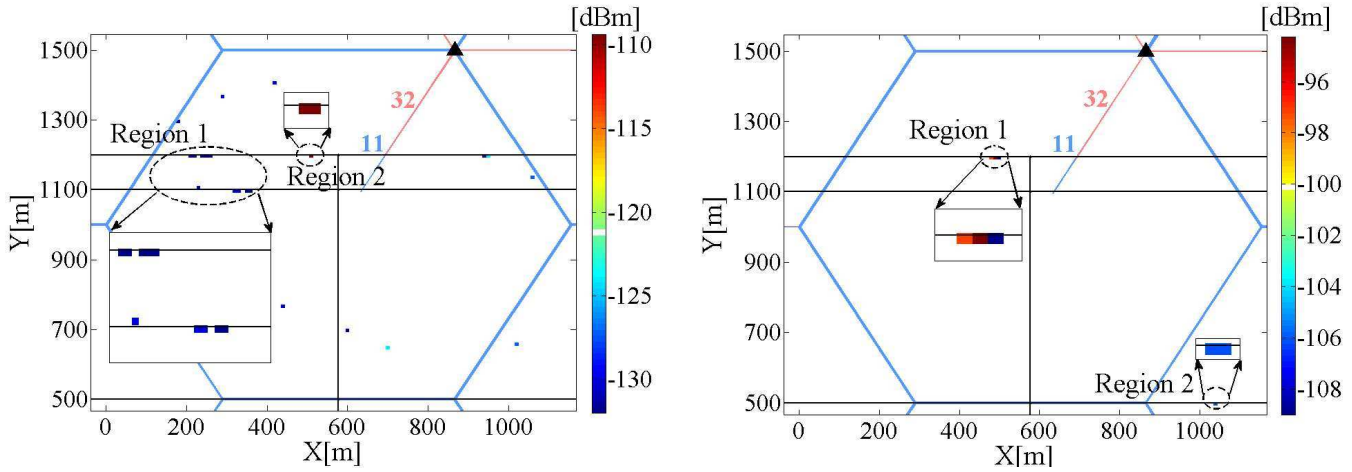

(a) Optimized value of $S_c^{(\text{thr}),\Omega(\text{a}_i)}$ in dBm for each area a_i of cell $c = 11$.

(b) Optimized value of $T_{c,c_0}^{(\text{thr}),\Omega(\text{a}_i)}$ in dBm for each area a_i of cell $c = 11$ with respect to target cell $c_0 = 32$.

Fig. 9. The optimized values of $S_c^{(\text{thr}),\Omega(\text{a}_i)}$ and $T_{c,c_0}^{(\text{thr}),\Omega(\text{a}_i)}$ thresholds for each area a_i of cell $c = 11$ with respect to target cell $c_0 = 32$. Speed of UEs on streets is 60 km/h.

in region 1 and 2 have $S_c^{(\text{thr}),\Omega(\text{a}_i)}$ values which are lower and higher, respectively, than the default one. Thus, the LB inter-RAT MRO algorithm has reacted on TLH-S and UHs of different areas simultaneously which is not possible for CPS MRO paradigm. Similarly, Fig. 9(b) shows that areas in region 1 and 2 have $T_{c,c_0}^{(\text{thr}),\Omega(\text{a}_i)}$ values which are higher and lower, respectively, than the default one. This also indicates that the LB MRO algorithm has reacted on different types of mobility failures in cell 11, i.e., TEH and TLH-T, even though they occur with respect to the same target cell 32.

VIII. Conclusion

In this paper, we have presented a new MRO paradigm for the inter-RAT handover thresholds in SON. The new paradigm classifies the mobility failure events per small areas and configures the UEs with specific handover thresholds depending on their locations in the network. As a result, the new paradigm can mitigate mobility failures which the current cell-specific and cell-pair specific MRO paradigms fail to resolve and boost the performance of inter-RAT MRO.

References

[1] C. Brunner, A. Garavaglia, M. Mittal, M. Narang, and J. Bautista, "Inter-system handover parameter optimization," in *IEEE Vehicular Technology Conference*, September 2006.

[2] 3GPP, "Self-configuring and self-optimizing network use cases and solutions," TR 36.902, Sophia-Antipolis, France, Tech. Rep., 2009.

[3] A. Awada, B. Wegmann, I. Viering, and A. Klein, "A SON-based algorithm for the optimization of inter-RAT handover parameters," *accepted (minor revisions) by IEEE Transactions on Vehicular Technology, Special issue on SON*, August 2012.

[4] A. Awada, B. Wegmann, I. Viering, and A. Klein, "Cell-pair specific optimization of the inter-RAT handover parameters in SON," in *Proc. IEEE International Symposium on Personal, Indoor and Mobile Radio Communications*, September 2012.

[5] A. Awada, B. Wegmann, I. Viering, and A. Klein, "Performance comparison of signal strength and signal quality based inter-RAT MRO," in *Proc. IEEE International Symposium on Wireless Communication Systems*, August 2012.

[6] 3GPP TSG SA WG5, 32.425 CR 0089. [Online]. Available: www.3gpp1.org/ftp/tsg_sa/WG5_TM/TSGS5_79/Docs/S5-113108

[7] 3GPP, "Stage 2 description; technical specification," TS 36.300, Sophia-Antipolis, France, Tech. Rep., 2011.